

# Effect of Temperature on Aqueous Solutions of Pyrene-Labeled (Hydroxypropyl)cellulose

Françoise M. Winnik

Xerox Research Center of Canada, Mississauga, Ontario, Canada L5K 2L1.  
Received April 17, 1987; Revised Manuscript Received July 7, 1987

**ABSTRACT:** The fluorescence spectroscopy of pyrene-labeled (hydroxypropyl)cellulose in water was examined as a function of temperature from 25 to 65 °C. The intense excimer emission observed at 25 °C increased slightly from 25 to 35 °C then decreased sharply before the cloud point of the polymer. The results are interpreted in terms of changes in two different interactions of the polymer with water: the hydrophobic interactions between pyrene groups and the hydrogen bonding of water molecules with the polymer hydroxypropyl substituents. A large solvent isotope effect on the excimer emission intensity, turbidity measurements, and fluorescence measurements on a polymer with very low label incorporation give further support to this interpretation.

## Introduction

Cellulose ethers have a broad range of industrial applications. They are used as additives in materials such as paints, inks, papers, cosmetics, pharmaceuticals, foods, and ceramics.<sup>1</sup> They may function, for example, as thickeners, flow-control agents, release agents, film components, or liquid crystals. The solution properties of cellulose ethers are dictated mostly by the chemical structure of the ether moiety and by the degree of substitution of the cellulose, e.g., the number of ether groups per glucose unit. Ethylcellulose is soluble in organic solvents but insoluble in water. Other cellulose ethers are soluble in water, for example, methylcellulose, (hydroxyethyl)cellulose, (hydroxypropyl)cellulose, or (carboxymethyl)cellulose.<sup>2</sup> Some minor chemical modifications, however, can alter dramatically the solution properties of cellulosic ethers. A fascinating example of this effect is provided by a new class of compounds, the hydrophobically modified cellulose ethers, in which long-chain hydrocarbon groups are attached covalently to a small number of hydroxyalkyl groups. These materials are soluble in water, but they exhibit an anomalous, large increase in solution viscosity which has been attributed to intermolecular associations of the alkyl chains.<sup>3</sup>

Aqueous solutions of certain cellulosic ethers undergo heat-induced phase changes. The changes depend primarily on the chemical structure of the ether group and on the degree of substitution of the cellulose hydroxyl groups. For example, (hydroxyethyl)cellulose is soluble in cold and hot water; methylcellulose forms gels when heated in water; (hydroxypropyl)cellulose (HPC) precipitates from water upon heating. This last behavior is not unique to cellulose ethers. It is encountered with other water-soluble polymers such as poly(ethylene oxides) and polyoxyethylated nonionic surfactants.<sup>4</sup> When an aqueous solution of (hydroxypropyl)cellulose is heated it suddenly becomes cloudy at a characteristic temperature, referred to as the "cloud point" or lower critical solution temperature (LCST). The phenomenon is reversible: upon cooling the cloudy suspension becomes clear at the same temperature.

Although attaching a small fraction of fluorescent groups is often thought of as a process which causes little or no change in the properties of a polymer, in the case of HPC even a very small level of substitution of hydrophobic groups affects the solubility of the polymer in water. This is the situation with pyrene-labeled (hydroxypropyl)cellulose (HPC-Py) (Figure 1). The synthesis of this polymer has been reported previously.<sup>5</sup> In this paper the effect of

heat on the spectroscopic properties of aqueous solutions of HPC-Py is described. Information was obtained by monitoring the UV absorption, steady-state fluorescence emission, and time-resolved fluorescence of the pyrene label as a function of temperature. Polymers with two different levels of pyrene incorporation were examined in order to assess the influence of hydrophobic substituents on the solution properties of HPC during the transition taking place at its lower critical solution temperature. Some experiments were carried out in H<sub>2</sub>O and in D<sub>2</sub>O, since it has been reported previously that hydrophobic interactions in the two solvents are markedly different.<sup>6</sup> Solvent isotope effects were observed on the cloud points and on the fluorescence emission of pyrene-substituted polymers.

## Experimental Section

**Materials.** (Hydroxypropyl)cellulose (HPC, Klucel L, Hercules) was purchased from Aldrich Chemical Co. The manufacturer's literature claims a molecular weight of 100 000. Other groups report measurements consistent with this value. One recent reference reports  $M(\text{sedimentation}) = 82\,000$ ,<sup>7a</sup> and another 73 000 with  $M_n = 36\,000$ .<sup>7b</sup> The pyrene-labeled (hydroxypropyl)cellulose samples were prepared by reaction of (hydroxypropyl)cellulose with 4-(1-pyrenyl)butyl tosylate in the presence of sodium hydride, following a procedure described in detail elsewhere.<sup>5</sup> The sample of high pyrene content (HPC-Py/56) was prepared using HPC (4.0 g), 4-(1-pyrenyl)butyl tosylate (0.50 g, 1.16 mmol), and sodium hydride (0.20 g, 60% dispersion on oil). The pyrene content of the final polymer (3.78 g), determined by UV analysis of a methanol solution using 4-(1-pyrene)butanol as a model, was calculated to be  $5.33 \times 10^{-5}$  mol/g of polymer, equivalent to one pyrene group per 56 glucose units for a polymer of  $M_n$  36 000. The sample of low pyrene content (HPC-Py/438) was prepared by using HPC (4.0 g), 4-(1-pyrene)butyl tosylate (60 mg, 0.14 mmol), and sodium hydride (0.10 g, 60% dispersion in oil). Its pyrene content was calculated to be  $6.8 \times 10^{-6}$  mol/g of polymer, equivalent to one pyrene group per 438 glucose units. The purity of the HPC-Py samples was important for the experiments described here. It was ascertained by GPC analysis using RI and UV detectors in tandem that the pyrene groups were covalently linked to the polymer and that low molecular weight pyrene impurities accounted for less than 0.1% of the total pyrene content. Water was deionized with a Millipore Milli-Q water purification system. D<sub>2</sub>O (99.8%) purchased from Merck, Sharp, and Dohme was used without purification.

**Spectroscopic Measurements.** UV absorption spectra were recorded with a Hewlett-Packard 8450A diode array spectrometer. For the peak to valley measurements the absorbances at minima and maxima were corrected to remove the light scattering effect by subtracting from these values the turbidity contribution calculated from the absorbance at 400 nm of the same sample. The peak to valley ratios were obtained by ratioing the corrected

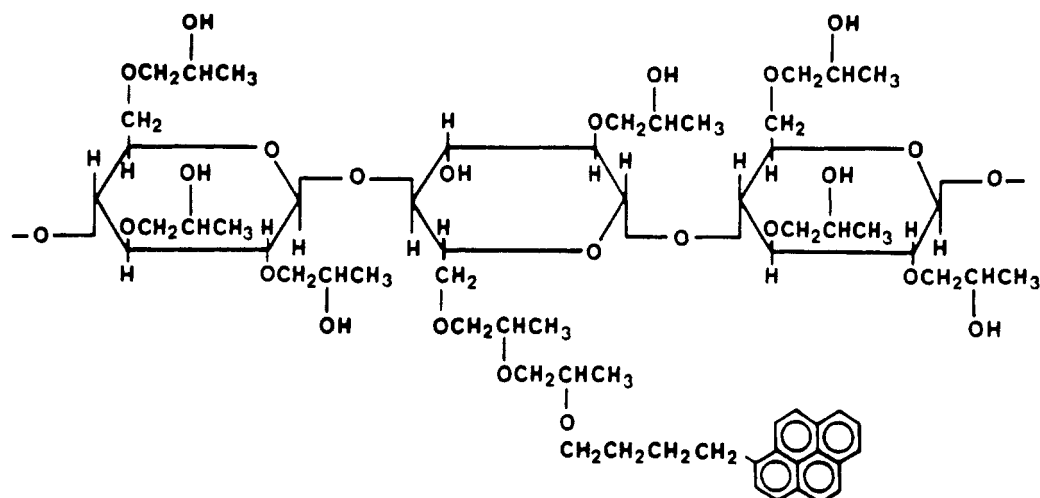


Figure 1. Idealized structure of pyrene-labeled (hydroxypropyl)cellulose.

absorbances at 344 and 337 nm. Temperature-controlled experiments were performed with a Hewlett-Packard 89100A temperature-control accessory consisting of a digitally controlled thermoelectrically heating and cooling cell holder with sample stirring capability and programmed temperature ramping. The temperature of the sample fluid was measured with a Hewlett-Packard 89102A Teflon-coated temperature sensing probe immersed in the sample fluid. The temperature of the fluid varied from 30 to 55 °C. Heating and cooling rates were chosen between 0.2 and 2 °C min<sup>-1</sup>. Steady-state fluorescence spectra were run on a SPEX Fluorolog 122 spectrometer equipped with a DM1B data system. Emission spectra were recorded by exciting at 335 nm. Excitation spectra were monitored in the ratio mode at 396 and 480 nm. The excitation and emission slits were set at 1 mm. Emission spectra were not corrected. Solutions were not degassed. It was determined previously that for aqueous solutions of HPC-Py emission intensities were unaffected by degassing. The excimer to monomer ratios were calculated by taking the ratio of the emission intensity at 480 nm to the half-sum of the emission intensities at 376 and 396 nm. It was verified that peak heights and peak areas were proportional. The temperature of the water-jacketted cell holder was controlled via a water circulating bath. It was not changed at a constant rate. After a desired temperature was reached the sample was allowed to equilibrate for 10 min. It took approximately 3 h to measure spectra from 25 to 70 °C. The temperature of the jacket was measured with a thermocouple. Fluorescence decay measurements were made with a home-built time-correlated single photon counting instrument.<sup>8</sup>

**Samples for Spectroscopic Analysis.** HPC-Py solutions were prepared at room temperature by allowing the polymer to swell and then dissolve. They were allowed to stand for 24 h before they were diluted to a known total volume. Solutions for UV/visible spectroscopy had concentrations ranging from 0.3 to 1.0 g L<sup>-1</sup>. The concentration of the samples for fluorescence analysis was 0.12 g L<sup>-1</sup> for HPC-Py/56 and 0.32 g L<sup>-1</sup> for HPC-Py/438.

**Cloud Point Determination.** The cloud points of aqueous solutions of HPC and pyrene-labeled HPC were determined by spectrophotometric detection of the changes in the turbidity of solutions heated at a constant rate in a magnetically stirred cell. The turbidity is equal to the absorbance of the solution at a wavelength where the sample does not absorb light. Pyrene has no absorption at wavelengths longer than 400 nm. For convenience the computer on the HP 8450A spectrometer was used to calculate the average absorbance between 400 and 800 nm. This average turbidity,  $\langle \tau \rangle$ , was plotted against the temperature of the solution. The points of sharp increase in turbidity on heating or sudden disappearance of turbidity on cooling were determined graphically. Unless stated otherwise the heating or cooling rates were set at 1 °C min<sup>-1</sup>. In this case the two values agreed within 0.5 °C, or less. The heating and cooling ramps were repeated at least twice for each solution. Values were reproducible within  $\pm 0.2$  °C. Values reported here are the temperatures corresponding to the appearance of turbidity upon heating.

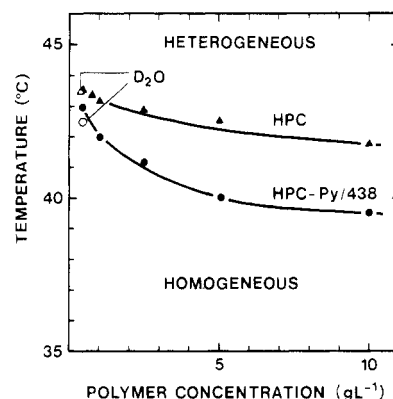


Figure 2. Phase diagram of the HPC-water and HPC-Py/438-water systems. Open symbols represent values measured in D<sub>2</sub>O.

**Samples for Measurements in D<sub>2</sub>O.** The polymer (HPC, HPC-Py/438, or HPC-Py/56, 10 mg) was dissolved in D<sub>2</sub>O (5 mL) overnight to effect the exchange of the hydroxylic protons. The solvent was removed by freeze-drying. Solutions for cloud point determinations were prepared from the exchanged polymer at concentrations of 0.3 g L<sup>-1</sup> for HPC and HPC-Py/438 and 0.15 g L<sup>-1</sup> for HPC-Py/56.

## Results

**Cloud Points of (Hydroxypropyl)cellulose and Pyrene-Labeled (Hydroxypropyl)cellulose.** In order to ensure the validity of the spectrophotometric determination of cloud points, HPC was examined first. Its cloud point was determined to be  $42.5 \pm 0.5$  °C for polymer concentrations higher than 5.0 g L<sup>-1</sup>, in agreement with reported values.<sup>9</sup> It increased to 43.5 °C for solutions of lower concentration (Figure 2). The cloud point of HPC-Py/438 was lower than that of HPC by approximately 2 °C for solutions of concentrations higher than 3.0 g L<sup>-1</sup>. As the polymer concentration decreases the cloud points of the two polymers increase and reach a value of 43.5 °C for solutions of 0.25 g L<sup>-1</sup> (250 ppm) (Figure 2). Accurate measurement of the cloud points of solutions of lower concentration was not possible: the solutions became only faintly turbid above the cloud point and the apparent onset of turbidity was not sharp.

An aqueous solution of a polymer with higher loading of pyrene, HPC-Py/56, was examined next. Surprising results were obtained. During heating an increase in turbidity occurred at temperatures well below the cloud point of HPC or HPC-Py/438. Turbidity reached a maximum at 41 °C, then with continuing heating the turbidity decreased to yield a nearly clear solution at 44

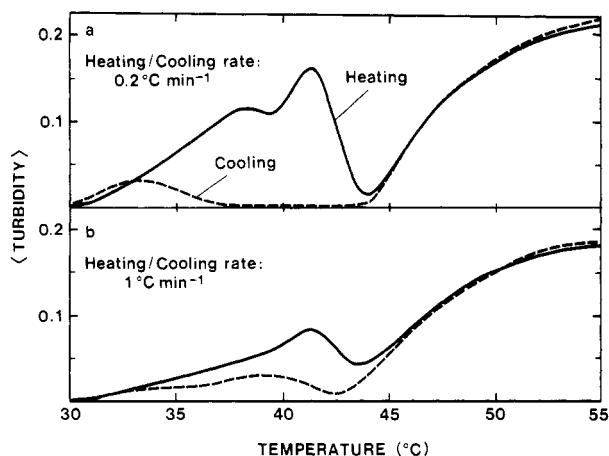


**Figure 3.** Changes in average turbidity of an aqueous solution of HPC-Py/56 ( $0.4 \text{ g L}^{-1}$ ) as a function of temperature. Heating/cooling rate:  $0.2 \text{ }^{\circ}\text{C min}^{-1}$  (a),  $1.0 \text{ }^{\circ}\text{C min}^{-1}$  (b); (—) heating ramp, (---) cooling ramp.

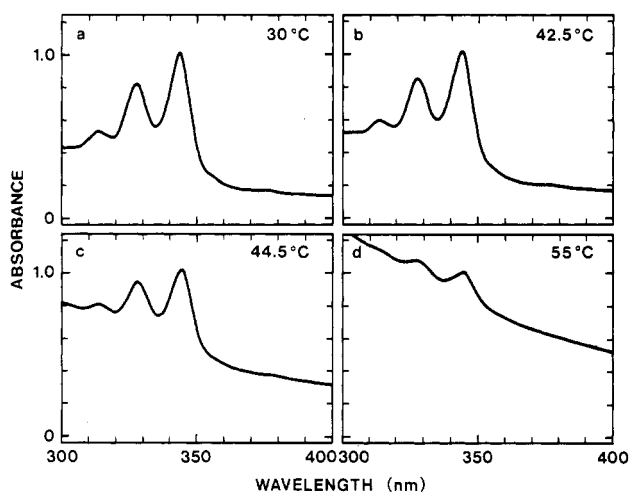


**Figure 4.** UV absorption spectra of aqueous solutions of HPC-Py/438 ( $0.32 \text{ g L}^{-1}$ ) normalized at  $343 \text{ nm}$ , measured at the following temperatures:  $30$  (a),  $42.5$  (b),  $44.5$  (c), and  $55$   $^{\circ}\text{C}$  (d).

$^{\circ}\text{C}$ . Above this point the turbidity of the solution increased monotonically. When a slower heating rate ( $0.2 \text{ }^{\circ}\text{C min}^{-1}$ ) was used, qualitatively similar changes in turbidity occurred, but the increase in turbidity below  $44 \text{ }^{\circ}\text{C}$  was amplified (Figure 3). The changes in turbidity were identical during heating and cooling in the  $44\text{--}55 \text{ }^{\circ}\text{C}$  temperature range but not for temperatures below  $44 \text{ }^{\circ}\text{C}$ . In this range, the turbidity observed during the heating cycle was not detected during the cooling cycle. The overall cycle behavior, however, was reproduced exactly when a sample was subjected to several consecutive heating/cooling cycles or when samples of different concentrations were examined. Because of the complexity of the temperature effect on the solutions of HPC-Py/56, it is difficult to define a cloud point for this polymer. The temperature of the second onset of turbidity occurred between  $43$  and  $44 \text{ }^{\circ}\text{C}$  for polymer concentrations of  $0.8$  to  $0.1 \text{ g L}^{-1}$ . This value or "apparent cloud point" is similar to the cloud points of HPC and HPC-Py/438 in this concentration range.

**Pyrene Absorption Spectra.** The absorption spectrum of pyrene in solutions of HPC-Py/438 and HPC-Py/56 was measured at several temperatures during the heating and cooling ramps. Representative spectra of HPC-Py/438 are shown in Figure 4. In the  $300\text{--}400\text{-nm}$  range pyrene exhibits three absorption peaks at  $308$ ,  $328$ , and  $344 \text{ nm}$ . At  $30 \text{ }^{\circ}\text{C}$  these peaks are well resolved. Pyrene does not absorb light of wavelength longer than

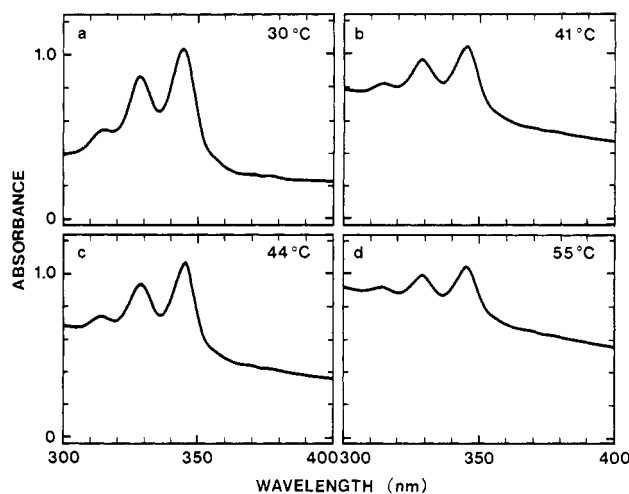


**Figure 5.** UV absorption spectra of aqueous solutions of HPC-Py/56 ( $0.40 \text{ g L}^{-1}$ ) normalized at  $343 \text{ nm}$ , measured at the following temperatures:  $30$  (a),  $41$  (b),  $44$  (c), and  $55$   $^{\circ}\text{C}$  (d).

$390 \text{ nm}$ , but it can be seen in Figure 4a that the solution of HPC-Py/438 has some absorbance at longer wavelength. This may be attributed to light scattering by small polymeric aggregates. The spectrum of the HPC-Py/438 solution does not change appreciably in the temperature range  $30\text{--}42 \text{ }^{\circ}\text{C}$ , as evidenced by a spectrum taken at  $42.5 \text{ }^{\circ}\text{C}$  (Figure 4b). However, as the temperature exceeds the cloud point the solution exhibits an increase in the absorbance due to light scattering and a broadening of the pyrene absorption bands (Figure 4c). At  $55 \text{ }^{\circ}\text{C}$  the effect of light scattering is predominant (Figure 4d). A qualitative indication of band broadening is the ratio of peak to valley intensities. However, since both light scattering by polymer aggregates and light absorption by the pyrene chromophore contribute to the total absorbance of the sample it was difficult to determine this ratio.<sup>10</sup>

The temperature effect on the absorption spectrum of pyrene in HPC-Py/56 is more complex, corroborating the observations made during cloud point determinations. Spectra taken at  $30$ ,  $41$ ,  $44$ , and  $55 \text{ }^{\circ}\text{C}$  are represented in parts a–d of Figure 5, respectively. At  $30 \text{ }^{\circ}\text{C}$  the spectrum of pyrene exhibits the same features as HPC-Py/438 with an identical peak to valley ratio of  $2.20$  for the band centered at  $344 \text{ nm}$ . As the temperature of the solution increases, changes in the spectrum occur. At  $41 \text{ }^{\circ}\text{C}$ , turbidity is more pronounced. Broadening of the pyrene absorption bands is also observed. At  $44 \text{ }^{\circ}\text{C}$  a decrease of the absorbance at  $400 \text{ nm}$  occurs, indicating a decrease of sample turbidity. At  $55 \text{ }^{\circ}\text{C}$  the absorption bands of the pyrene chromophore appear very broad. The absorbance due to light scattering is predominant.

**Pyrene Fluorescence Spectra. Steady-State Measurements.** At  $25 \text{ }^{\circ}\text{C}$  in water HPC-Py/56 shows an emission due to locally excited pyrene chromophores (intensity  $I_M$ , "monomer" emission) with the  $[O,O]$  band located at  $376 \text{ nm}$  and a broad emission centered at  $480 \text{ nm}$  due to pyrene excimer (intensity  $I_E$ ). The ratio of the excimer to monomer intensities is  $0.49$ . As the temperature increases the following events occur: First the ratio of excimer to monomer emission intensities increases and reaches a maximum of  $0.55$  at  $35 \text{ }^{\circ}\text{C}$ . Then the ratio decreases sharply to reach its limiting value of  $0.21$  at  $50 \text{ }^{\circ}\text{C}$ . The midpoint of the transition is  $\sim 42 \text{ }^{\circ}\text{C}$  (Figure 6). The decrease in the excimer emission intensity is accompanied by a shift of the excimer emission maximum from  $480$  to  $472 \text{ nm}$  at  $55 \text{ }^{\circ}\text{C}$ .

Next the changes in  $I_E/I_M$  were followed as a function of decreasing temperature from  $55$  to  $25 \text{ }^{\circ}\text{C}$  (Figure 6). In

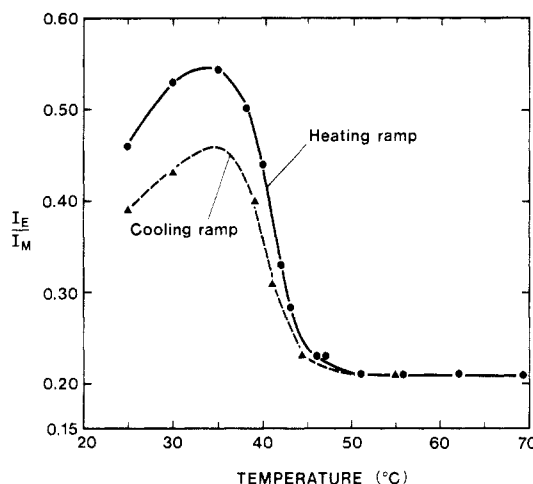


**Figure 6.** Excimer to monomer emission intensities ratio ( $I_E/I_M$ ) as a function of temperature for a solution of HPC-Py/56 ( $0.12 \text{ g L}^{-1}$ ); (●) values measured during heating, (▲) values measured during cooling.

**Table I**  
Fluorescence Decay Measurements

temp, °C	monomer		excimer	
	$\tau$ , ns	prefactor	$\tau$ , ns	prefactor
25	$\tau_1$ 34	0.30	$\tau_1$ 3.5	0.64
	$\tau_2$ 115	0.70	$\tau_2$ 84	0.36
54	$\tau_1$ 39	0.35	$\tau_1$ 3.3	0.55
	$\tau_2$ 118	0.64	$\tau_2$ 80.6	0.45
	$\chi^2$ 1.51		$\chi^2$ 1.70	

this case a sharp increase of the ratio was observed, with the midpoint of the transition occurring at  $\sim 41^\circ\text{C}$ . The ratio reached a maximum value at  $35^\circ\text{C}$ . At all temperatures lower than  $50^\circ\text{C}$ , the  $I_E/I_M$  ratio measured during the cooling ramp was smaller than that measured during the heating ramp. When the cooled sample was kept at  $25^\circ\text{C}$  for several hours, its emission spectrum became identical with that of a solution which had not been subjected to the heating-cooling treatment. This hysteresis parallels the results of the turbidity measurements.

Changes in temperature were also accompanied by small changes in the pyrene excitation spectra. At  $25^\circ\text{C}$  the excitation spectra for the monomer and the excimer are similar in shape but the former is blue-shifted by approximately 3 nm, with maxima at 342.5 and 345.5 nm, respectively. This situation remained unchanged as the temperature of the sample was increased to  $42^\circ\text{C}$ , but above this temperature both excitation spectra gradually underwent small shifts in opposite directions. At  $55^\circ\text{C}$  the maxima of the excitation spectra for monomer and excimer are separated by only 1 nm, e.g., 343.5 nm for the monomer and 344.5 nm for the excimer.

The fluorescence emission spectrum of HPC-Py/438 in water at  $25^\circ\text{C}$  also presents both a monomer and an excimer emission. But in this case the excimer emission at  $25^\circ\text{C}$  is much weaker. The changes in this ratio with increasing temperature are qualitatively similar to those observed for HPC-Py/56, but their magnitude is much weaker. The ratio of excimer to monomer emission intensities varied from 0.06 at  $25^\circ\text{C}$  to 0.04 at  $70^\circ\text{C}$ , with a maximum value of 0.07 at  $39^\circ\text{C}$ .

**Pyrene Fluorescence Decay Measurements.** The pyrene fluorescence decay was measured at 25 and  $54^\circ\text{C}$  for an aqueous solution of HPC-Py/56 (see Table I). It was surprising to observe that, qualitatively, the fluorescence decay results were not influenced strongly by temperature. The most important result is that neither at 25

$^\circ\text{C}$  nor at  $54^\circ\text{C}$  was it possible to detect a rising component in the excimer profile. This implies that at both temperatures most of the pyrene excimer arises from preformed ground-state aggregates of pyrene groups and that the excimer forms faster than resolution of the instrument (1 ns). The excimer decay both at 25 and at  $54^\circ\text{C}$  shows two components, a short component (3 ns) and a longer component. The monomer decays at both temperature are nonexponential as well. They are reported as a sum of two exponential terms. Heterogeneity in the distribution of the pyrene label along the polymer backbone may account for the complexity of the pyrene monomer decay.

**Measurements in  $\text{D}_2\text{O}$ .** Cloud points of the three polymers were measured at only one concentration each. To minimize the amount of residual water the measurements were performed on solutions of polymers in which the hydroxylic protons had been exchanged with deuterons. Both HPC and HPC-Py/438 exhibited very well-defined cloud points at the concentration chosen ( $0.3 \text{ g L}^{-1}$ ). The cloud point of HPC was not affected by the change in solvent, while the cloud point of HPC-Py/438 was slightly lower in  $\text{D}_2\text{O}$  than in water (Figure 2). The behavior of HPC-Py/56 was quite different. At room temperature its solubility was much lower in  $\text{D}_2\text{O}$  than in  $\text{H}_2\text{O}$ . The turbidity of the  $\text{D}_2\text{O}$  solution increased slowly from the beginning of the heating ramp ( $30^\circ\text{C}$ ) up to about  $47^\circ\text{C}$  where it reached a plateau. The changes were reversible upon cooling. They were not affected significantly by changes in heating rate from 1 to  $0.2^\circ\text{C min}^{-1}$ .

Substitution of the solvent from  $\text{H}_2\text{O}$  to  $\text{D}_2\text{O}$  also caused significant changes in the fluorescence spectra of HPC-Py/56. The most obvious change was a drastic reduction of the pyrene excimer intensity when HPC-Py/56 was dissolved in  $\text{D}_2\text{O}$ . The ratio  $I_E/I_M$  dropped from a value of 0.49 in  $\text{H}_2\text{O}$  at  $25^\circ\text{C}$  to 0.12 in  $\text{D}_2\text{O}$  at  $25^\circ\text{C}$ .

## Discussion

Water is an unusual solvent for (hydroxypropyl)cellulose. This situation is emphasized in an empirical fashion by the large difference in Hildebrand solubility parameter between water ( $\delta = 23.4$ ) and HPC for which a value of  $\sim 10.7$  was determined by viscosity and surface tension measurements.<sup>12</sup> Normally a polymer is soluble only in liquids having solubility parameter values within the range  $\delta \pm 3.0$ . The unusual aqueous solubility of HPC has been attributed to the formation of hydrogen bonds between water and the propylene glycol chains of the polymer which render the enthalpy of mixing of HPC in water ( $\Delta H_m$ ) negative.<sup>13</sup> Hydrogen bonding between the polymer and water triggers a change of the water structure around the polymer. A layer of highly organized water molecules is created around the polymer. This circumstance results in an unfavorable negative entropy of mixing. At room temperature the free energy of mixing remains negative despite the negative entropy because of the favorable enthalpy contribution. At higher temperatures the entropic term becomes more important and the enthalpy of dissolution becomes less favorable as a result of the thermal lability of the hydrogen bonds. At the LSCT the free energy of dissolution becomes positive; a polymer-rich phase precipitates. At this temperature thermal expansion of the solvent prevents the formation of hydrogen bonds between water molecules and the polymer, which does not expand as much as the solvent. Intrapolymeric hydrogen bonds form and attractive forces between polymer chains are prevalent ( $\Delta H_m \geq 0$ ). Similar thermodynamic considerations apply to the case of polymers substituted with hydrophobic groups as discussed in the next sections.

When HPC bears a very small number of pyrene groups

as in HPC-Py/438 the dissolution of the polymer in water is not altered significantly. A small lowering of the LSCT is observed. This may reflect either a slightly less favorable enthalpic contribution or a more negative entropic contribution. Fluorescence measurements show that the majority of the pyrene chromophores are isolated from each other. They are probably located in hydrophobic cavities within the polymer.

A noticeable change in the properties of aqueous solutions occurs when the level of pyrene substitution is increased. In the sample HPC-Py/56 (1 pyrene per 56 glucose units) there is an average of two pyrenes per chain. Fluorescence studies have ascertained that a large fraction of the pyrene substituents form ground-state dimers or aggregates. Water is the only solvent in which such aggregates have been observed. It is postulated here that the formation of pyrene dimers is favorable in water as a result of hydrophobic interactions.<sup>14,15</sup> Unlike the HPC backbone, a pyrene substituent cannot undergo hydrogen bonding with water. The number of hydrogen bonds between water molecules which are disrupted or distorted by the nonpolar pyrene groups is minimized if two or more pyrenes come in close proximity. The nonpolar dimers are then surrounded by a cage of highly organized water molecules bound tightly by strong hydrogen bonds. The formation of a dimer through hydrophobic interaction between two nonpolar groups in water has a positive entropy and a positive enthalpy. The entropic term is dominating, rendering the free energy of dimer formation favorable (negative) at room temperature. At a certain temperature the free energy of pyrene dimer formation becomes positive, the pyrene dimers are then broken, and the water molecules from the clusters around them reorganize with bulk water. Since labeling of HPC was done randomly there are many possible arrangements of pyrene dimers. It is not surprising that the pyrene dimers break over a broad temperature range, in contrast to the precipitation of the polymer which occurs at a specific temperature.

This interpretation of the interpolymeric interactions was deduced from the following two salient features of the pyrene fluorescence: (1) Pyrene excimer emission originates from preformed ground-state aggregates, and (2) the value of  $I_E/I_M$  decreases with increasing temperature, this decrease reflecting an increase of pyrene monomer emission intensity at the expense of excimer emission. The total emission (from pyrene monomer and excimer) remains approximately constant over this temperature range. The turbidity measurements of HPC-Py/56 solutions showed the formation of polymeric aggregates at temperatures lower than the cloud point of the polymer. Already at room temperature aggregates of HPC-Py/56 exist. Their formation is promoted by the hydrophobic interactions between pyrenes of different polymer chains. As the temperature increases, pyrene dimers are broken, triggering changes in polymer association. It is not unexpected that the size of aggregates fluctuates as these phenomena occur. Changes in the pyrene fluorescence reflect events happening on a molecular scale. The turbidity measurements on the other hand sense changes on a scale larger than 1000 Å. Can the results of the two types of measurements be correlated? One comparison is suggested in Figure 7, where the monomer intensity and the turbidity of an aqueous solution of HPC-Py/56 are plotted together as a function of temperature. One notices immediately that the temperature of onset of polymer precipitation (44 °C), indicated by a sharp increase in turbidity, corresponds to the point of leveling-off of pyrene

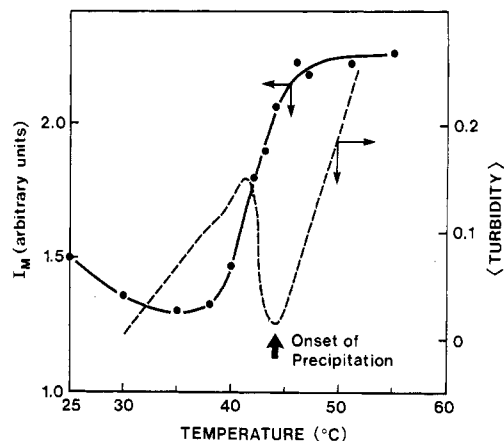


**Figure 7.** Pyrene monomer emission intensity ( $I_M$ ) as a function of temperature for a solution of HPC-Py/56 in water ( $0.12 \text{ g L}^{-1}$ ) and average turbidity of a solution of HPC-Py/56 in water ( $0.40 \text{ g L}^{-1}$ ) as a function of temperature (heating rate,  $0.2 \text{ }^\circ\text{C min}^{-1}$ ).

monomer intensity. This suggests that separation of the pyrene dimers takes place before the precipitation of the polymer and the number of residual pyrene dimers in the precipitated polymer remains constant up to 60 °C.

In the precipitated polymer the pyrene excimer still originates mostly from ground-state pyrene dimers or aggregates as vouched for both by the absence of an excimer rising component in the time-resolved experiments and by the differences observed in the excitation spectra of monomer and excimer. There may be subtle changes in the ground-state pyrene dimer geometry, as suggested by a small shift of the excimer emission maximum from 480 nm at 25 °C to 472 nm at 55 °C. The wavelength of maximum emission for excimer fluorescence is known to depend on the separation and orientation of chromophores in bi-chromophoric compounds.<sup>16</sup> It might also be affected by environmental effects due to changes in polymer conformation accompanying the polymer precipitation.<sup>17</sup>

The solvent isotope effect on the pyrene fluorescence emission of HPC-Py/56 corroborates the proposed description, if one accepts the premise that hydrophobic interactions are weaker in  $\text{D}_2\text{O}$  than in  $\text{H}_2\text{O}$ , as suggested first by Némethy and Scheraga<sup>18</sup> and discussed in detail by Ben-Naim.<sup>6,19</sup> The effect of  $\text{D}_2\text{O}$  on the  $I_E/I_M$  ratio is substantial. In fact the hydrophobic interactions between pyrene groups are almost precluded in  $\text{D}_2\text{O}$ . In this solvent the nonpolar pyrene groups cannot be accommodated through dimer formation, which results in a lowering of the solubility of HPC-Py/56 in  $\text{D}_2\text{O}$  compared to  $\text{H}_2\text{O}$ .

## Conclusion

The effect of temperature on the solubility of (hydroxypropyl)cellulose and pyrene-labeled (hydroxypropyl)cellulose in water was monitored by measuring the changes in turbidity of polymeric solutions and the spectroscopy of the pyrene label. At low labeling the solubility of the polymer in water is characteristic of that of HPC itself. At higher labeling the solubility of the polymer in water is altered. Significant aggregation of the polymer takes place at temperatures lower than the polymer cloud point through the formation of pyrene dimers or higher aggregates. The pyrene dimers are stabilized by hydrophobic interactions in water. These interactions are made more labile than the hydrogen bonds between water and the polymer backbone by increasing temperature. A pronounced solvent isotope effect on the pyrene fluorescence emission stresses the importance of hydrophobic interactions between pyrene groups below the lower critical solution temperature.

**Acknowledgment.** I thank Dr. A. J. Paine for GPC measurements, Dr. K. Sienicki for fluorescence decay measurements, and Professor M. A. Winnik for the use of the SPEX fluorescence spectrometer in his laboratory and for many stimulating discussions.

**Registry No.** HPC, 9004-64-2.

## References and Notes

- (1) Just, E. K.; Majewicz, T. G. *Encyclopedia of Polymer Science and Engineering*, 2nd ed.; Wiley: New York, 1985; Vol 3, pp 226-269.
- (2) See, for example: *Handbook of Water-soluble Gums and Resins*; Davidson, R. L., Ed.; McGraw Hill: New York, 1980.
- (3) Gelman, R. A.; Barth, H. G. *Water-soluble Polymers*; Glass, J. E., Ed.; ACS Symp. Ser. 213; American Chemical Society: Washington, DC, 1986; p 101.
- (4) Bailey, F. E., Jr.; Callard, R. W. *J. Appl. Polym. Sci.* **1956**, *1*, 56. Weckström, K.; Zulauf, M. *J. Phys., Colloq.* **1984**, *45*, C7-137.
- (5) Winnik, F. M.; Winnik, M. A.; Tazuke, S.; Ober, C. K. *Macromolecules* **1987**, *20*, 38.
- (6) Ben-Naim, A.; Wilf, J.; Yaacobi, M. *J. Phys. Chem.* **1973**, *77*, 95.
- (7) (a) Webowyj, R. S.; Gray, D. G. *Macromolecules* **1984**, *17*, 1512. (b) Nystrom B.; Bergman, R. *Eur. Polym. J.* **1978**, *14*, 431.
- (8) Martinho, J.; Egan, L. S.; Winnik, M. A. *Anal. Chem.* **1987**, *59*, 861.
- (9) *Klucel*, a booklet distributed by the manufacturer, Hercules, Inc., Wilmington, DE 19894. Furusawa, K.; Tagawa, T. *Colloids Polym. Sci.* **1985**, *263*, 353.
- (10) The total absorbance can be corrected for light scattering contributions as follows: (1) if one assumes that the light scattering contribution is proportional to  $\lambda^{-4}$ , one can subtract this contribution from the total absorbance; (2) one can use a log-log plot as described previously.<sup>11</sup> Both methods gave a value of 2.2 for the ratio of the peak (344 nm) to the valley (336 nm) of the pyrene absorption of aqueous solutions of HPC-Py/56 at temperatures between 25 and 45 °C. At higher temperatures scattering effects are too prominent for meaningful measurements of this ratio.
- (11) For a similar treatment, see: Leach, S. J.; Scheraga, H. A. *J. Am. Chem. Soc.* **1960**, *82*, 4790.
- (12) Roberts, G. A. F.; Thomas, J. M. *Polymer* **1978**, *19*, 459.
- (13) Samuels, R. G. *J. Polym. Sci.* **1969**, *16*, 201.
- (14) Ben-Naim, A. *Hydrophobic Interactions*, Plenum: New York, 1980.
- (15) Tanford, C. *The Hydrophobic Effect: Formation of Micelles and Biological Membranes*; Wiley: New York, 1980.
- (16) Zachariasse, K. A.; Kühnle, W. Z. *Phys. Chem. N. F.* **1976**, *101*, 267.
- (17) Lakowicz, J. R. *Principles of Fluorescence Spectroscopy*; Plenum: New York, 1983; Chapter 7.
- (18) Némethy, G.; Scheraga, H. A. *J. Chem. Phys.* **1964**, *41*, 680.
- (19) Marcus, Y.; Ben-Naim, A. *J. Chem. Phys.* **1985**, *83*, 4744.

## Two-Dimensional NMR of Polysaccharides: Spectral Assignments of Cellulose Triesters

Charles M. Buchanan,\* John A. Hyatt, and Douglas W. Lowman

Research Laboratories, Eastman Chemicals Division, Eastman Kodak Company, P.O. Box 1972, Kingsport, Tennessee 37662. Received February 27, 1987

**ABSTRACT:** The combined use of homonuclear and heteronuclear two-dimensional NMR has provided the first unambiguous spectral assignment for the polymer backbone of cellulose triacetate, cellulose tripropionate, and cellulose tributyrate. Simple techniques have been applied which allow enhancement of the resolution in the one-dimensional spectra of these polysaccharides. Data are presented which suggest that the solution macromolecular conformation for cellulose esters is sensitive to both solvent polarity and size of acyl substituent.

## Introduction

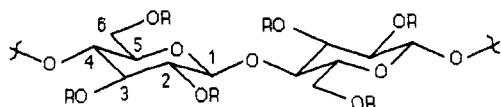
In the past 10 years, NMR techniques have routinely been applied to the study of cellulose esters.<sup>1</sup> In all of these reports, spectral assignments were made by chemical derivatization or by comparison to spectra of mono- or oligosaccharides. Moreover, due to line broadening and small differences in chemical shifts, much of the information potentially available from coupling patterns was lost. As part of our work in cellulose esters, we required unambiguous spectral assignments and simple techniques for improving resolution in one-dimensional (1D) spectra. The work presented here has provided complete spectral assignments for the polymer backbone of cellulose triacetate (CTA, 1), cellulose tripropionate (CTP, 2), and cellulose tributyrate (CTB, 3). We have also found that in many

cases, significant spectral enhancement can be obtained in the 1D spectra by application of a Lorentzian to Gaussian transformation with a suitable weighting constant. The data suggest that the solution macromolecular conformation of cellulose esters is sensitive to both solvent polarity and size of acyl substituent.

## Results and Discussion

**Chemical Shift Assignments.** In analogy to the methods developed for NMR studies of oligosaccharides,<sup>2</sup> peptides,<sup>3</sup> and other polymeric systems,<sup>4</sup> an effective strategy for shift assignments of polysaccharides is through two-dimensional (2D) homonuclear and heteronuclear chemical shift correlation spectroscopy. The method allows assignment of proton resonances from the evidence of proton-proton connectivities which are then correlated with the resonances in the carbon-13 NMR spectrum. This process is demonstrated for CTA (1) (CDCl<sub>3</sub>).

Figure 1a shows the 1D <sup>1</sup>H NMR spectrum of the ring region of CTA (1), to which resolution enhancement has been applied (vide infra). The coupling information contained in this spectrum and the <sup>1</sup>H-<sup>1</sup>H connectivities in the homonuclear chemical shift correlation spectrum (COSY, Figure 2) permitted a straightforward assignment of the proton spectrum of CTA (1).



- 1 R = OAc
- 2 R = OPr
- 3 R = OBu